ORGAN TOXICITY AND MECHANISMS

# Protection by chrysin, apigenin, and luteolin against oxidative stress is mediated by the Nrf2-dependent up-regulation of heme oxygenase 1 and glutamate cysteine ligase in rat primary hepatocytes

**Chin-Shiu Huang · Chong-Kuei Lii · Ai-Hsuan Lin · Yu-Wen Yeh · Hsien-Tsung Yao · Chien-Chun Li · Tsu-Shing Wang · Haw-Wen Chen**

**Abstract** Chrysin, apigenin, and luteolin are flavones that differ in their number of hydroxyl groups in the B ring. In this study, we investigated the protection by chrysin, apigenin, and luteolin against *tert*-butyl hydroperoxide (tBHP)-induced oxidative stress and the possible mechanisms involved in rat primary hepatocytes. Chrysin, apigenin, and luteolin dose-dependently up-regulated the protein expression of heme oxygenase 1 (HO-1) and glutamate cysteine ligase (GCL) catalytic (GCLC) and modifier subunit (GCLM) and increased the intracellular glutathione (GSH) content and the ratio of GSH to oxidized GSH. Among the flavones studied, chrysin showed the greatest induction of HO-1, GCLC, and GCLM protein expression and GSH content. Cellular reactive oxygen species production induced by tBHP was attenuated by pretreatment with chrysin, apigenin, and luteolin ($P < .05$), and this protection was reversed by the GCL inhibitor l-buthionine-S-sulfoximine and the HO-1 inhibitor zinc protoporphyrin. Chrysin, apigenin, and luteolin activated extracellular signal-regulated protein kinase 2 (ERK2), nuclear factor erythroid 2-related factor 2 (Nrf2) nuclear translocation, nuclear Nrf2–antioxidant responsive element (ARE) binding activity, and ARE-dependent luciferase activity. Both ERK2 and Nrf2 siRNAs attenuated chrysin-induced HO-1, GCLC, and GCLM protein expression. Taken together, these results suggest that chrysin, apigenin, and luteolin inhibit tBHP-induced oxidative stress by up-regulating HO-1, GCLC, and GCLM gene transcription via the ERK2/Nrf2/ARE signaling pathways in rat primary hepatocytes.

**Keywords** Extracellular signal-regulated protein kinase 2 (ERK2) · Flavones · Heme oxygenase 1 (HO-1) · Glutamate cysteine ligase (GCL) · Nuclear factor erythroid 2-related factor 2 (Nrf2)

Chin-Shiu Huang and Chong-Kuei Lii have contributed equally to this work.

C.-S. Huang
Department of Health and Nutrition Biotechnology, Asia University, Taichung, Taiwan, ROC

C.-K. Lii · Y.-W. Yeh · H.-T. Yao · H.-W. Chen (✉)
Department of Nutrition, China Medical University, Taichung, Taiwan, ROC
e-mail: chenhw@mail.cmu.edu.tw

A.-H. Lin · C.-C. Li
Department of Nutrition, Chung Shan Medical University, Taichung, Taiwan, ROC

T.-S. Wang (✉)
Department of Biomedical Sciences, Chung Shan Medical University, Taichung, Taiwan, ROC
e-mail: tsushing@csmu.edu.tw

T.-S. Wang
Department of Medical Research, Chung Shan Medical University Hospital, Taichung, Taiwan, ROC

## Introduction

Flavonoids are polyphenolic compounds that are ubiquitous in nature and are categorized into flavonols, flavones, flavanones, isoflavones, catechins, anthocyanidins, and chalcones. Over 9,000 flavonoids have been identified, and they are present in fruits, vegetables, and beverages. Recently, flavonoids have attracted considerable attention because of their versatile physiological functions, including

antioxidation, anti-inflammation, anti-atherosclerosis, anti-cancer, hypolipidemia, and hypoglycemia effects (Xiao et al. 2011). One of the working mechanisms for these actions of flavonoids lies in the fact that flavonoids activate the transcription factor nuclear factor erythroid-derived 2-related factor (Nrf2) and up-regulate the expression of genes encoding antioxidant and phase II detoxification enzymes, including heme oxygenase 1 (HO-1), glutamate cysteine ligase (GCL), glutathione (GSH) reductase, GSH S-transferase (GST), and NAD(P)H:quinone oxidoreductase (Dinkova-Kostova and Talalay 2010; Lee et al. 2010; Mulcahy et al. 1997; Yang et al. 2010). Among these enzymes, HO-1 and GCL have attracted great attention because of their therapeutic potential in diabetes, cancer, AIDS, and neurodegenerative and liver diseases (Abraham and Kappas 2008; Kim et al. 2011; Franklin et al. 2009).

HO-1 catalyzes the first and rate-limiting step of free heme degradation into biliverdin, carbon monoxide, and free ferrous iron (Ryter et al. 2002). It is an antioxidant enzyme that is strongly induced by various stimuli, including its substrate heme, oxidative stress, the signaling proteins (nerve growth factor, tumor necrosis factor $\alpha$, and interleukin-1), and bioactive phytochemicals (Boyle et al. 2011; Choi and Kim 2008; Salinas et al. 2003; Terry et al. 1999; Wu et al. 2006; Wung et al. 2006). Humans and mice with HO-1 mutation exhibit a serious impairment of iron metabolism that leads to liver and kidney oxidative damage and inflammation (Tracz et al. 2007; Saikawa et al. 2000). Moreover, transgenic mice deficient in HO-1 of an apoli-poprotein E null background exhibit more advanced atherosclerotic lesion formation in response to a Western diet (Yet et al. 2003).

GCL catalyzes the first and rate-limiting step in de novo GSH synthesis. GCL is composed of two subunits, the heavy catalytic subunit GCLC (73 kDa) and the light modifier subunit GCLM (31 kDa) (Gipp et al. 1992, 1995). The expression of GCLC and GCLM is regulated primarily at the transcriptional level; however, a post-transcriptional mechanism such as mRNA stability has also been reported to be involved (Liu et al. 1998; Song et al. 2005). Multiple cis-acting response elements, including antioxidant responsive element (ARE) and activator protein 1 (AP-1) binding sites, have been identified in the 5′-flanking regulatory region of the human GCLC and GCLM genes (Gipp et al. 1995; Moinova and Mulcahy 1998). Because of the important role of GSH in cellular redox homeostasis, animals defective in GCLM are highly susceptible to oxidative stress (Kann et al. 2005).

Nrf2 belongs to the NF-E2 family of basic leucine zipper redox-sensitive transcription factors. Under basal conditions, Nrf2 is retained in the cytoplasm by Kelch-like ECH-associated protein 1 (Keap1), which acts as a substrate adapter of a Cullin 3-based E3 ubiquitin ligase complex and results in rapid degradation of Nrf2 through the proteasome pathway (Itoh et al. 1999). The Nrf2-Keap1 complex is disrupted in response to oxidant and electrophilic stress, which leads to the translocation of free Nrf2 into the nucleus, where it forms a heterodimer with small Maf and binds to the ARE of target genes. The ARE is identified in the promoter of many genes encoding antioxidant and detoxifying enzymes, including GCLC, GCLM, HO-1, NAD(P)H:quinone oxidoreductase 1, UDP-glucuronyl transferase, and GST (Alam et al. 1999; Ikeda et al. 2004; Kalthoff et al. 2010; Shenvi et al. 2009; Yang et al. 2011). Therefore, Nrf2 is recognized as an important regulator in cytoprotection against prooxidant and chemical insult.

Chrysin, apigenin, and luteolin are members of the flavonoids (Lopez-Lazaro 2009; Seelinger et al. 2008; Shukla and Gupta 2010) that differ in their number of hydroxyl groups in the B ring (Fig. 1). Although the biological functions of the flavones are well-known, few studies have investigated the potential of the flavones to activate cellular antioxidant and anti-inflammatory genes such as HO-1 and GCL and the specific transcription factor and upstream signaling kinases involved. The present study therefore aimed to investigate the effect of three flavones with different number of hydroxyl groups in the B ring, that is, chrysin, apigenin, and luteolin, on HO-1, GCLC, and GCLM expression in rat primary hepatocytes as well as the underlying mechanism involved. In addition, we aimed to determine the role of enhancement of antioxidant gene expression in protection against oxidant-induced oxidative stress.

## Materials and methods

Cell culture medium (RPMI-1640) and penicillin–streptomycin solution were from GIBCO-BRL (Gaithersburg, MD, USA); Matrigel and ITS$^+$ (insulin, transferrin, selenium, BSA, and linoleic acid) were from Collaborative Biomedical Products (Bedford, MA, USA); fetal bovine serum was from HyClone (Logan, UT, USA); collagenase type I was from Worthington Biochemical (Lakewood, NJ, USA); TRIzol reagent was from Invitrogen (Carlsbad, CA, USA); chrysin, apigenin, luteolin, dexamethasone, HEPES, and l-buthionine-S-sulfoximine (BSO) were from Sigma Chemical (St. Louis, MO, USA); and zinc protoporphyrin (ZnPP) was from Calbiochem (La Jolla, CA, USA). Small interfering RNAs (siRNAs) against Nrf2 and ERK2 were purchased from Dharmacon (Lafayette, CO, USA).

Hepatocyte isolation and culture

Male Sprague–Dawley rats (weighing 250–300 g) were purchased from the National Animal Breeding and Research

**Fig. 1** Structures of chrysin, apigenin, and luteolin



**A** Chrysin    **B** Apigenin    **C** Luteolin
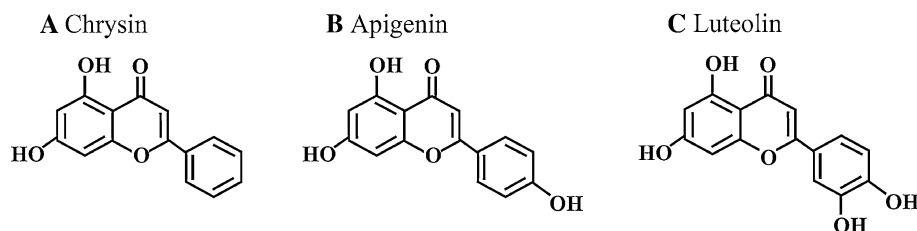
Center (Taipei, Taiwan). Hepatocytes were isolated by a modification of the two-step collagenase perfusion method described previously (Yang et al. 2011). After isolation, hepatocytes ($3 \times 10^6$ cells/dish) were plated on collagen-coated 60-mm plastic tissue dishes in RPMI-1640 medium (pH 7.38) supplemented with 10 mM HEPES, 1 % ITS$^+$, 1 μM dexamethasone, 100 IU penicillin/ml, and 100 μg streptomycin/ml. Cells were incubated at 37 °C in a 5 % $CO_2$ humidified incubator. After 4 h, the cells were washed with phosphate-buffered saline (PBS) to remove any unattached or dead cells, and the same medium supplemented with 0.1 μM dexamethasone was added. Twenty hours after attachment, cells were treated with various concentrations (5–25 μM) of chrysin, apigenin, or luteolin.

MTT assay

Cell viability was assessed by measuring the ability of viable cells to reduce a yellow 3-(4,5-dimethylthiazol-2-yl)-2,5-diphenyltetrazolium bromide (MTT) to a purple formazan by mitochondrial succinate dehydrogenase. After incubation with each flavone for 24 h, the medium was removed, and hepatocytes were then incubated in RPMI-1640 medium containing 0.5 mg/ml MTT for 4 h. The medium was then removed, and isopropanol was added to dissolve the formazan. The absorbance was read at 570 nm in an ELISA reader; absorbance in cells treated with 0.1 % dimethyl sulfoxide (DMSO) was regarded as 100 % cell viability. The cell viability was greater than 90 % after exposure to up to 50 μM of each flavone (data not shown).

Determination of cellular reactive oxygen species

Detection of intracellular reactive oxygen species (ROS) was performed by using the probe 2,7-dichlorofluorescin diacetate (H$_2$DCF-DA; Molecular Probes Inc., Eugene, OR, USA). Hepatocytes were pretreated with chrysin, apigenin, or luteolin for 24 h before being challenged with 0.5 mM *tert*-butyl hydroperoxide (tBHP) for 1 h. To assess the effect of the inhibitors BSO (a GCL inhibitor) and ZnPP (an HO-1 inhibitor), cells were pretreated with the respective inhibitor for 2 h before the addition of chrysin, apigenin, or luteolin. As a control, an equal amount of DMSO was added to untreated cells. The treated cells were washed twice with PBS to remove the extracellular compounds, and H$_2$DCF-DA (5 μmol/l) was added. The fluorescence was then detected with a confocal microscope (Leica TCS SP2).

Measurement of intracellular reduced and oxidized GSH content

After treatment with chrysin, apigenin, or luteolin for 24 h, 100 μl of the cytosolic fraction of hepatocytes was reacted with 200 μl of 10 mM Ellman's reagent by gentle mixing, which was followed by the addition of 60 μl of 20 % 5-sulfosalicylic acid to cause acid precipitation. After centrifugation at $10,000 \times g$ and 4 °C for 10 min, 100 μl of supernatant was used to analyze reduced and oxidized GSH content by the use of an HPLC–MS (Hewlett Packard) (Yao et al. 2011).

SDS-PAGE and Western blotting

Cells were washed twice with cold PBS and were harvested in 500 μl of 20 mM potassium phosphate buffer (pH 7.0). Cell homogenates were centrifuged at $9,000 \times g$ for 30 min at 4 °C. The resulting supernatant was then ultracentrifuged at $105,000 \times g$ for 1 h at 4 °C. The protein content of the cytosolic and microsomal fraction was measured by using the Coomassie Plus protein assay kit (Pierce Chemical Company, Rockford, IL, USA). Equal amounts of proteins were electrophoresed in a SDS-polyacrylamide gel, and proteins were then transferred to polyvinylidene fluoride membranes. The nonspecific binding sites in the membranes were blocked with 5 % nonfat dry milk in 15 mM Tris-150 mM NaCl buffer (pH 7.4) at 4 °C overnight. After blocking, membranes were probed with anti-GCLC and anti-GCLM (Abcam), anti-HO-1 (Calbiochem), anti-Nrf2 (Santa Cruz), anti-ERK, anti-phospho-ERK (Thr202/Tyr204), anti-p38, anti-phospho-p38 (Thr180/Tyr 182), anti-Akt, anti-phospho-Akt, anti-PARP (Cell Signaling Technology), anti-GAPDH (Millipore), and anti-actin (Sigma) antibodies. The membranes were then probed with the secondary antibody labeled with horseradish peroxidase. The bands were visualized by using an enhanced chemiluminescence kit (PerkinElmer Life Science, Boston, MA, USA) and were scanned by a luminescent image

analyzer (FUJIFILM LAS-4000, Japan). The bands were quantitated with ImageGauge software.

## RNA isolation and RT-PCR

Total RNA was extracted by using TRIzol reagent. RNA extracts were suspended in nuclease-free water and were frozen at $-20$ °C until the RT-PCR analysis was performed (Yang et al. 2011). The sequences for the RT-PCR primers were as follows: for HO-1 (forward: 5′-AG CATGTCCCAGGATTTGTC-3′; reverse: 5′-AAGGCGG TCTTAGCCTCTTC-3′), GCLC (forward: 5′-CCTTCT GGCACAGCACGTTG-3′; reverse: 5′-TAAGACGGCA TCTCGCTCCT- 3′), GCLM (forward: 5′- CTGACATT GAAGCCCAGGA-3′; reverse: 5′-ACATTGCCAAACCA CCACA-3′), and glyceraldehyde 3-phosphate dehydrogenase (GAPDH) (forward: 5′-CCATCACCATCTTCCAG GAG-3′; reverse: 5′-CCTGCTTCACCACCTTCTTG-3′). The PCRs for HO-1 and GAPDH were performed as follows: 5 min at 95 °C and 25 cycles for 30 s at 94 °C, 45 s at 56 °C, and 45 s at 72 °C. For GCLC amplification, the PCR cycle number was 32 times through a 60-s denaturing step at 94 °C, a 60-s annealing step at 60 °C, and a 90-s elongation step at 72 °C. For GCLM, the PCR cycle number was 35 times through a 15-s denaturing step at 95 °C, a 30-s annealing step at 62 °C, and a 45-s elongation step at 72 °C. The GAPDH cDNA level was used as the internal standard. PCR products were resolved in a 1 % agarose gel and were scanned by using a Digital Image Analyzer (Alpha Innotech) and quantitated with Image-Gauge software (FUJIFILM Science Lab). The PCR amplicons were then electrophoresed in 1 % agarose gels containing $1\times$ TAE buffer (40 mM Tris/20 mM glacial acetic acid/2 mM EDTA).

## Transient transfection and luciferase activity assay

pGL3-2xARE/Luc fragment containing two tandem repeats of double-stranded oligonucleotides spanning the Nrf2 binding site, 5′-TGACTCAGCA-3′, was kindly provided by Dr. Being-Sun Wung (National Chiayi University, Taiwan). Cells were transiently transfected for 8 h with 0.4 μg of the pGL3-2xARE/Luc vectors by using nano-fectin reagent (PAA, Pasching, Austria) and were then changed to fresh medium for 2 h before being exposed to various concentrations of chrysin, apigenin, or luteolin for an additional 24 h. The luciferase activity was measured by using a luciferase substrate solution (Promega, Madison, WI, USA) and was corrected on the basis of $\beta$-galactosidase activity. The value for cells treated with 0.1 % DMSO (control) was set at 1.

## Electrophoretic mobility shift assay

After each experiment, cells were washed twice with cold PBS and were then scraped from the dishes with 1,000 μl of PBS. Cell homogenates were centrifuged at $2,000\times g$ for 5 min. The cell pellet was allowed to swell on ice for 15 min after the addition of 200 μl of hypotonic buffer (pH 7.4) containing 10 mM HEPES, 10 mM KCl, 1 mM $MgCl_2$, 1 mM EDTA, 0.5 mM DTT, 0.5 % Nonidet P-40, 4 μg/ml leupeptin, 20 μg/ml aprotinin, and 0.2 mM phenylmethylsulfonyl fluoride. After centrifugation at $6,000\times g$ for 15 min, pellets containing crude nuclei were resuspended in 50 μl of hypertonic buffer (pH 7.4) containing 10 mM HEPES, 400 mM KCl, 1 mM $MgCl_2$, 1 mM EDTA, 0.5 mM DTT, 10 % glycerol, 4 μg/ml leupeptin, 20 μg/ml aprotinin, and 0.2 mM phenylmethylsulfonyl fluoride at 4 °C for 30 min. The nuclear extracts were then obtained by centrifugation at $10,000\times g$ for 15 min and were frozen at $-80$ °C.

Electrophoretic mobility shift assay (EMSA) was performed according to our previous study (Cheng et al. 2004). The Light-ShiftTM chemiluminescent EMSA kit (Pierce Chemical) and synthetic biotin-labeled double-stranded rHO-1 ARE consensus oligonucleotides (forward: 5′-AACCA<u>TGACACAGCA</u>TAAAA-3′; reverse: 5′-TTT TA<u>TGCTGTGTCA</u>TGGTT-3′) were used to measure Nrf2 nuclear protein–DNA binding activity. Unlabeled double-stranded rHO-1 ARE oligonucleotide and a mutant double-stranded oligonucleotide (5′-AACCAgtcCACAGCATA AAA-3′) were used to confirm the protein-binding specificity. The nuclear protein and DNA complex was separated by electrophoresis on a 6 % Tris–borate-EDTA-polyacrylamide gel and was then electrotransferred to a Hybond-N$^+$ nylon membrane. The nuclear protein–DNA bands were developed by using an enhanced chemiluminescence kit (Thermo).

## RNA interference by small interfering RNA

Hepatocytes were transiently transfected for 24 h with 50 nM each of ERK2 or Nrf2 siRNA SMARTpool by using DharmaFECT transfection reagents (Thermo, Rockford, IL, USA) according to the manufacturer's instructions. The 4 siRNAs against the rat ERK2 gene are (1) ACACU AAUCUCUCGUACAU, (2) AAAAUAAGGUGCCGUG GAA, (3) UAUACCAAGUCCAUUGAUA, and (4) UC GAGUUGCUAUCAAGAAA. The 4 siRNAs against the rat Nrf2 gene are (1) GAACACAGAUUUCGGUGAU, (2) AGACAAACAUUCAAGCCGA, (3) GGGUUCAGUGA CUCGGAAA, and (4) AGAAUAAAGUUGCCGCUCA. A nontargeting control-pool siRNA was also tested and was used as the negative control. After 24 h of transfection,

cells were treated with chrysin for another 24 h. Cell samples were collected for Western blotting analysis.

## Determination of flavone concentrations in medium

Each flavone at a concentration of 25 μM was added in the culture medium for 24 h in the absence or presence of hepatocytes. The percentage of chrysin, apigenin, and luteolin remaining in the medium at different time intervals was then determined. Aliquots of 100 μl of culture medium were taken and mixed with an equal volume of ice-cold methanol containing 1 % ascorbic acid and 1 % formic acid. The samples were then centrifuged at $10,000 \times g$ for 20 min. The resulting supernatant was used for analysis of the remaining of flavonoids by LC/MS.

The flavones were identified by their retention times, compared with those of the reference standards, in the LC/MS system (Yao et al. 2011). In the HPLC–MS system, an Agilent Zorbax Eclipse XDB-C8 column (5 μm, 150 × 3.0 mm i.d.) was used. The isocratic system consisted of 60 % solvent A (10 mM ammonia acetate containing 0.5 % formic acid) and 40 % solvent B (acetonitrile containing 0.5 % formic acid), which were used to separate the tested compounds. The flow rate was 0.6 ml/min. Data acquisition was performed by using selected ion monitoring. Ions representing negative species of the compounds were selected, and peak areas were measured. The retention times of chrysin, apigenin, and luteolin were 5.5, 2.6, and 2.1 min, respectively. The percentage of flavonoids remaining was calculated by dividing the peak area of the tested time point in the incubation by that of the 0 time point.

## Statistical evaluation

Data were analyzed by using one-way analysis of variance (SAS Institute, Cary, NC, USA). The significance of the difference among group means was determined by Tukey's test; $P$ values $<0.05$ were taken to be statistically significant.

## Results

### Flavones induce GCLC, GCLM, and HO-1 expression

After treatment with 0–25 μM of flavones for 24 h, the protein expression of GCLM and HO-1 increased dose-dependently with chrysin, apigenin, and luteolin ($P < .05$) (Fig. 2a). Levels of GCLC protein were dose-dependently induced by chrysin and luteolin ($P < .05$), but not by apigenin. A dose–response effect of these flavones was also observed on HO-1 mRNA expression, and 25 μM of these
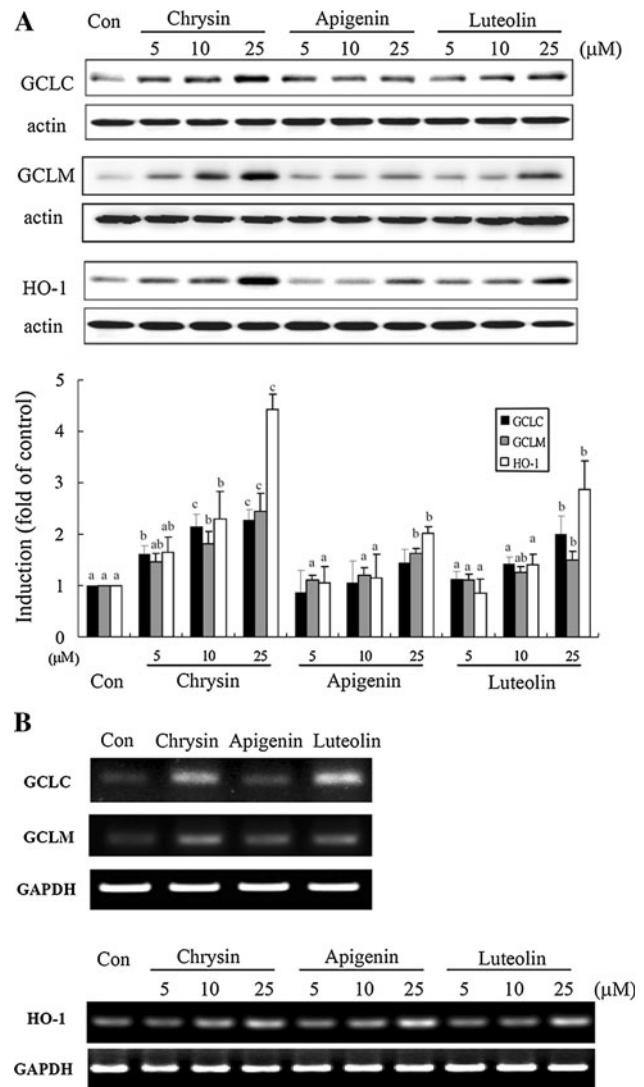


**Fig. 2** Flavones induce the expression of GCLC, GCLM, and HO-1. Rat primary hepatocytes were treated with 0–25 μM chrysin, apigenin, or luteolin for 24 h. **a** Protein and **b** mRNA levels were measured by immunoblotting and RT-PCR, respectively. For GCLC and GCLM mRNA, cells were treated with 25 μM chrysin, apigenin, or luteolin. Results are presented as mean ± SD of three independent experiments. Results not sharing the *same letter* are significantly different ($P < .05$)

flavones induced GCLC and GCLM mRNA expression (Fig. 2b).

### Chrysin, apigenin, and luteolin increase total GSH and the ratio of GSH to oxidized GSH

Owing to the increase of GCLC and GCLM expression by chrysin, apigenin, and luteolin, we next determined the effect of these flavones on cellular GSH content. After 24 h of treatment, chrysin, apigenin, and luteolin significantly increased the total cellular GSH level (Fig. 3a), and chrysin had a greater GSH-increasing effect than did apigenin or
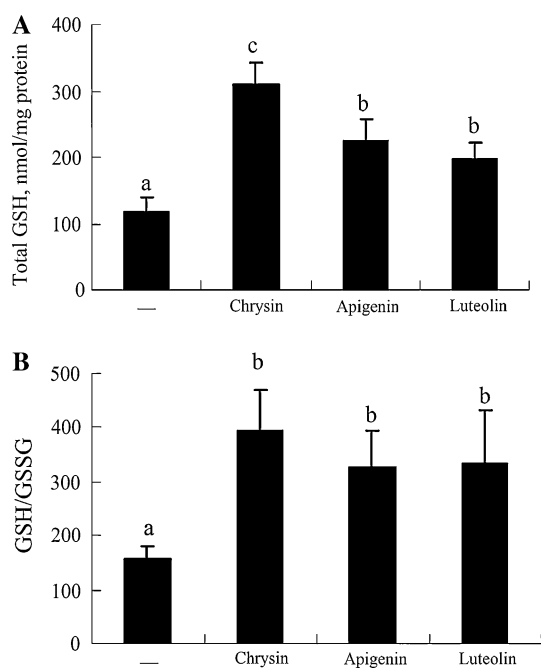
**A**



**B**

**Fig. 3** Chrysin, apigenin, and luteolin increase **a** total cellular GSH content and **b** the GSH/GSSG ratio. Hepatocytes were incubated with 25 μM chrysin, apigenin, or luteolin for 24 h. GSH and oxidized GSH (GSSG) were determined by HPLC/MS. Total GSH = reduced GSH + 2 × GSSG. Results are presented as mean ± SD of three independent experiments. Results not sharing the *same letter* are significantly different ($P < .05$)

luteolin ($P < .05$). In addition, these flavones significantly increased the ratio of GSH to oxidized GSH (GSH/GSSG) compared with that in the control group ($P < .05$) (Fig. 3b). These findings suggested that chrysin, apigenin, and luteolin enhance GSH synthesis and improve GSH redox status.

ERK2 and Nrf2 activation with flavone induction of GCLC, GCLM, and HO-1 expression

Next, we investigated the effect of chrysin on Nrf2 activation, which plays an important role in the up-regulation of antioxidant and phase II detoxification enzyme gene expression. With 25 μM chrysin, we observed a time-dependent increase in Nrf2 nuclear translocation up to 6 h (Fig. 4a). In contrast with the increase in nuclear Nrf2 by chrysin, the amount of Nrf2 in the cytosolic fraction was decreased. As shown by EMSA, 10 and 25 μM of chrysin, apigenin, and luteolin enhanced the binding activity of the ARE consensus sequences to nuclear proteins (Fig. 4b).

Furthermore, we used cells transfected with luciferase reporter constructs harboring the ARE to determine the specificity of chrysin, apigenin, and luteolin for this sequence. As shown in Fig. 4c, luciferase activity was significantly increased by treatment with 25 μM of these flavones ($P < .05$). In addition, we examined the role of

Nrf2 in the induction of HO-1, GCLC, and GCLM protein expression by chrysin by using an siRNA SMARTpool system to create an Nrf2-knockdown model. The knockdown efficiency of the Nrf2 siRNA SMARTpool system was confirmed by immunoblotting assay. With knockdown of Nrf2 expression, the increase in nuclear Nrf2 and the induction of GCLC, GCLM, and HO-1 protein expression by chrysin were apparently attenuated (Fig. 4d).

Nrf2 activation is known to be under the regulation of several kinases, including mitogen-activated protein kinases (MAPKs), phosphatidylinositol 3-kinase (PI3K)/Akt, and protein kinase C. We next investigated whether MAPKs and Akt were involved in the chrysin-induced Nrf2 activation and antioxidant gene expression. Compared with the control group, ERK2 activation was observed in response to chrysin treatment, and maximal activation was noted at 6 h (Fig. 5a). However, no activation of p38 or Akt was found.

To confirm the role of ERK2 in chrysin-induced Nrf2 nuclear translocation, ERK2 silencing was performed by an siRNA transfection approach. As shown in Fig. 5b, ERK2 silencing ablated the chrysin-activated Nrf2 nuclear translocation and suppressed chrysin-induced HO-1, GCLC, and GCLM protein expression.

Flavones attenuate tBHP-induced oxidative damage through the induction of HO-1 and GCL

To test whether the up-regulation of HO-1, GCLC, and GCLM expression by flavones offers antioxidant protection to hepatocytes, tBHP was used as a prooxidant to induce oxidative stress. Cells were pretreated with 25 μM of chrysin, apigenin, or luteolin for 24 h, followed by exposure to 0.5 mM tBHP for an additional 1 h. Compared with that in the control group, tBHP exposure significantly induced cellular ROS formation ($P < .05$) (Fig. 6). Cells pretreated with chrysin, apigenin, and luteolin, however, showed significantly lower ROS formation than did cells treated with tBHP alone ($P < .05$). Furthermore, both the HO-1 inhibitor ZnPP and the GCL inhibitor BSO abolished the protection by chrysin against tBHP-induced oxidative stress. These findings suggested that the up-regulation of HO-1 and GCL by flavones explains, at least in part, the antioxidant activity of chrysin, apigenin, and luteolin.

Concentration changes in chrysin, apigenin, and luteolin during cell culture

In the absence of hepatocytes, chrysin, apigenin, and luteolin in culture medium remained relatively stable over 24 h (Fig. 7). The percentage remaining of chrysin, apigenin, and luteolin dropped quickly in the presence of hepatocytes, however. The mass spectrum of luteolin, apigenin, and chrysin was presented (Supplementary Fig. S1).
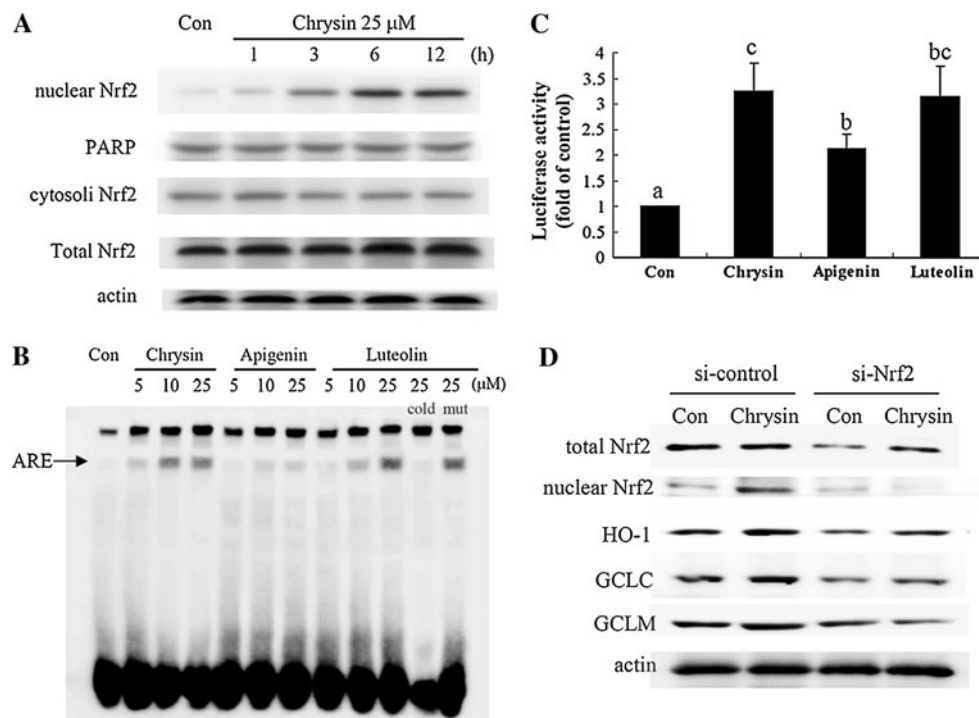
**Fig. 4** Flavones activate Nrf2. Cells were treated with 25 μM chrysin for the indicated time periods. **a** Immunoblots of nuclear, cytosolic, and total extracts from treated cells were then probed with the Nrf2-specific antibody. **b** Nuclear extracts of cells treated with 5, 10, and 25 μM chrysin, apigenin, or luteolin for 6 h were used to determine Nrf2 nuclear protein–DNA binding activity. A total amount of 4 μg protein was used for EMSA. To confirm the specificity of the nucleotide, cold probe (biotin-unlabeled Nrf2 binding site) and biotin-labeled double-stranded mutant Nrf2 oligonucleotide were included in the EMSA. **c** Hepatocytes were transfected with 2×ARE-luciferase construct (ARE) for 12 h and were then treated with 25 μM chrysin, apigenin, or luteolin for an additional 24 h. Induction is shown as an increase in the normalized luciferase activity in the treated cells relative to the control cells. Results are presented as mean ± SD of three independent experiments. Results not sharing the *same letter* are significantly different ($P < .05$). **d** After attachment, hepatocytes were transiently transfected with nontargeting control siRNA or siNrf2 for 24 h, followed by treatment with 25 μM chrysin for an additional 24 h. Total and nuclear Nrf2 and HO-1, GCLC, and GCLM expression were determined
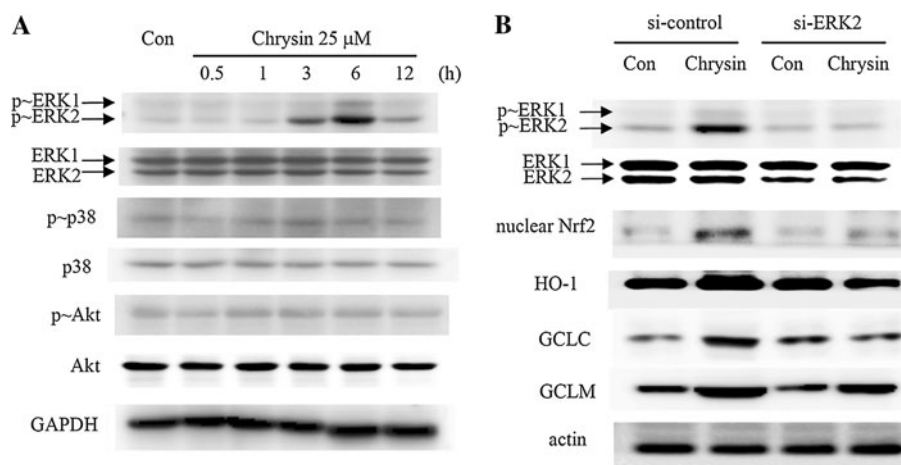


**Fig. 5** Effect of chrysin on ERK2 activation and the role of ERK2 in chrysin-induced HO-1, GCLC, and GCLM expression in rat primary hepatocytes. **a** Hepatocytes were incubated with 25 μM chrysin for various time periods. Cellular proteins were prepared for phosphorylated ERK1/2, p38, and Akt determination. **b** After attachment, cells were transiently transfected with nontargeting control siRNA or siERK2 for 24 h, followed by treatment with 25 μM chrysin for an additional 24 h. Cellular and nuclear proteins were used for Western blot analysis. siERK2 abolished chrysin-induced Nrf2 nuclear translocation and attenuated HO-1, GCLC, and GCLM protein expression
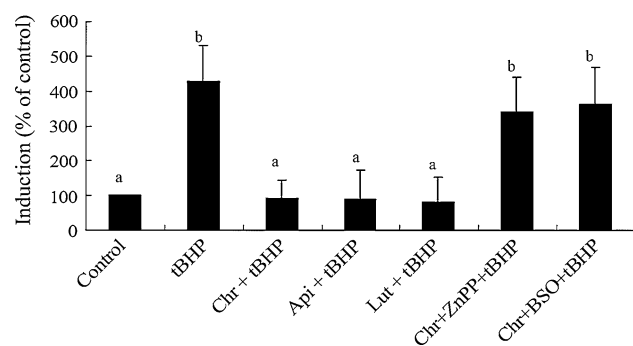
**Fig. 6** Flavones inhibit *tert*-butyl hydroperoxide (tBHP)-induced peroxide formation. Cells were pretreated with DMSO as the solvent control or 25 μM chrysin, apigenin, or luteolin for 24 h before being challenged with 0.5 mM tBHP for another 1 h. The HO-1 inhibitor ZnPP and the GLC inhibitor BSO were added 2 h before treatment with chrysin

After incubation with hepatocytes for 2 h, the percentage remaining of chrysin, apigenin, and luteolin was 24.5, 27.7, and 48.4 %, respectively. This may have been the result of quick uptake of flavones or metabolic degradation of flavones by hepatocytes.

## Discussion

Oxidative stress is a state representing a disturbance between antioxidation and prooxidation within cells. Under oxidative stress, cellular DNA, protein, and membrane unsaturated fatty acids are susceptible to oxidation, which leads to cell damage. This explains why enhancement of antioxidant defense capacity protects against ROS-related diseases, including atherosclerosis, carcinogenesis, and neurodegenerative diseases (Abraham and Kappas 2005; Biswas and Rahman 2009). In this study, we demonstrated that the flavones chrysin, apigenin, and luteolin inhibited tBHP-induced oxidative stress and that this suppression was likely associated with the up-regulation of HO-1, GCLC, and GCLM expression through the ERK2/Nrf2 pathway.

GSH is an endogenously synthesized tripeptide thiol, and GCL catalyzes the rate-limiting step in GSH synthesis (Franklin et al. 2009). GCL is a heterodimeric holoenzyme composed of GCLC and GCLM subunits (Gipp et al. 1992, 1995). Reduced GSH is the most abundant nonprotein thiol in mammalian cells and is the preferred substrate for several enzymes in xenobiotic metabolism and antioxidant defense (Lu 2009). Decreases in GSH concentration have been shown to be a common feature of many pathological conditions, including diabetes, AIDS, and neurodegenerative and liver diseases (Franco et al. 2007). Additionally, GSH was recently reported to modulate redox-sensitive components of signal transduction cascades involved in the regulation of gene expression, apoptosis, and cell proliferation (Biswas and Rahman 2009; Franco and Cidlowski 2009). In this study, chrysin, apigenin, and luteolin induced GCLC and GCLM mRNA and protein expression in rat primary hepatocytes (Fig. 2a, b). Consistent with the increase in GCLC and GCLM expression, a greater cellular GSH level and GSH/GSSG ratio were noted in flavone-treated cells (Fig. 3a, b). Moreover, we found that chrysin, apigenin, and luteolin significantly inhibited tBHP-induced ROS production (Fig. 6) and that this suppression was attenuated by the GCL inhibitor BSO. These results suggest that the protection against oxidative stress by chrysin, apigenin, and luteolin can be explained, at least in part, by their up-regulation of GCLC and GCLM gene transcription, which enhances GSH synthesis.

Accumulating evidence indicates that induction of HO-1 expression acts as an important protective mechanism against various chronic diseases, including atherosclerosis, diabetes, obesity, cardiovascular disease, and hypertension (Abraham and Kappas 2005, 2008). This protection is offered by the heme degradation products. Increased HO-1 expression and bilirubin accumulation protect against cytotoxicity induced by $H_2O_2$ in vascular smooth muscle cells and endothelial cells (Clark et al. 2000; Jansen et al. 2010). Hyperglycemia has been linked to oxidative stress, and streptozotocin-induced diabetic rats have significantly greater urinary output of 8-epi-isoprostane PGF2α, an indicator of overall oxidative stress. Diabetic rats receiving daily intraperitoneal injection of CORM-3, a carbon monoxide donor, exhibit a greater than sixfold increase in plasma carbon monoxide levels compared with rats receiving vehicle. Carbon monoxide significantly decreases the urinary output of 8-epi-isoprostane PGF2α in diabetic animals (Rodella et al. 2006). Acute administration of iron to intact rats (Aziz and Munro 1986) or to rat hepatoma cells (Rogers and Munro 1987) induces the synthesis of the iron-storage protein ferritin. Increased ferritin expression attenuates $H_2O_2$ and hemin-mediated cytotoxicity in porcine aorta endothelial cells (Balla et al. 1992). In our previous studies, we showed that induction of HO-1 expression by the diterpene lactone andrographolide and the flavonoids butein and phloretin suppresses tumor necrosis factor α-induced intercellular adhesion molecule 1 expression and tBHP-induced oxidative damage (Yang et al. 2011; Yu et al. 2010). Similar to the induction of GCLC and GCLM mentioned above, chrysin, apigenin, and luteolin dose-dependently induced HO-1 mRNA and protein expression in rat primary hepatocytes (Fig. 2a, b). In addition, the inhibition of tBHP-induced peroxide formation by chrysin, apigenin, and luteolin was attenuated by ZnPP (an HO-1 inhibitor) (Fig. 6). Our results thus suggest that the antioxidant activity of chrysin, apigenin, and luteolin is also associated with their induction of HO-1.

**Fig. 7** Concentration changes in flavones during hepatocyte culture. Chrysin, apigenin, and luteolin (25 µM) were added to the cell culture medium in the absence (*diamond*) or presence (*box*) of hepatocytes. Changes in **a** chrysin, **b** apigenin, and **c** luteolin concentrations in the medium over 24 h were determined by HPLC–MS. Values are mean ± SD of three independent experiments
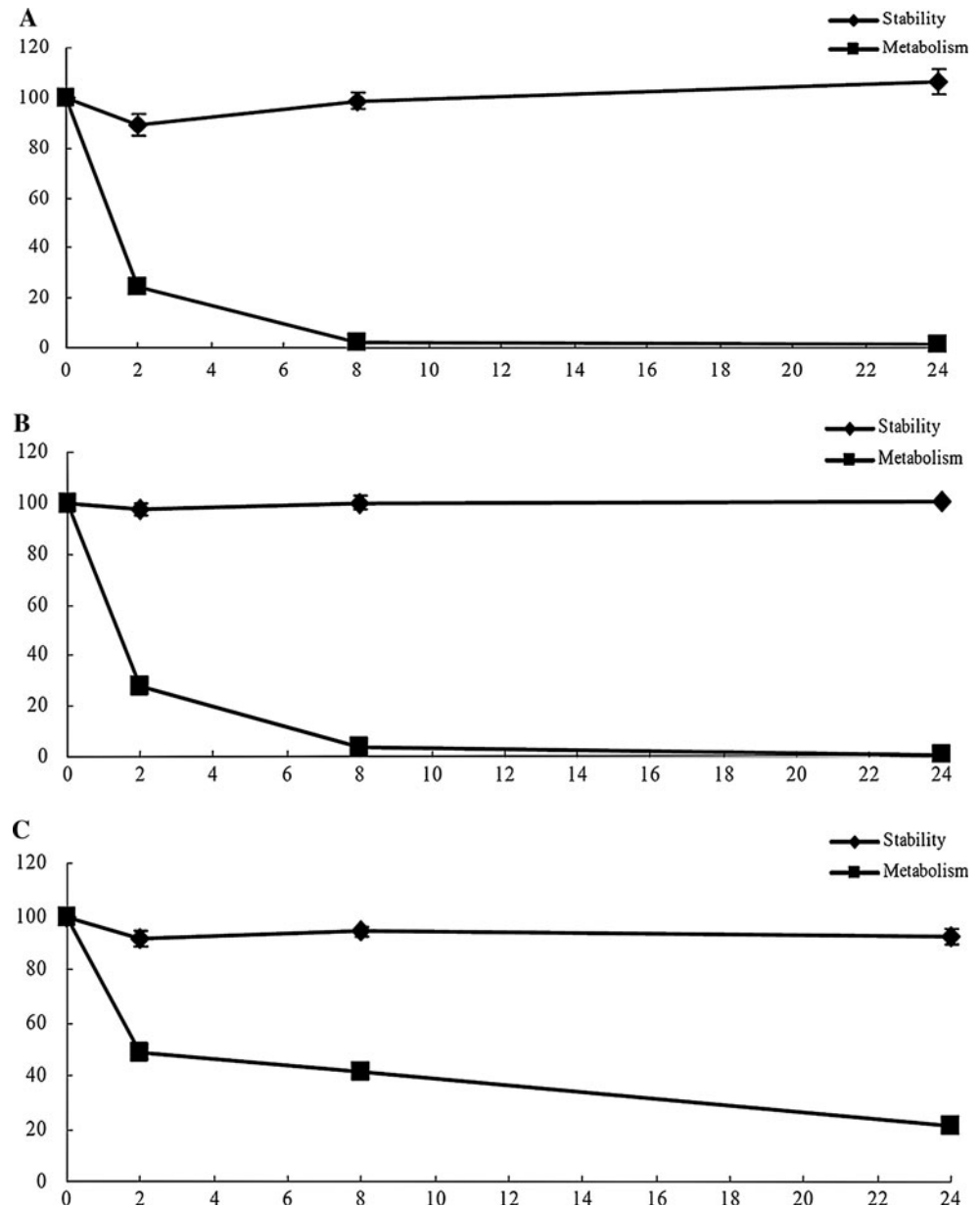


A variety of signaling pathways are involved in the induction of HO-1 and GCL transcription. Nrf2 is the transcription factor attracting most attention (Surh et al. 2008). It is well established that Nrf2 activation is under the regulation of protein kinase C, PI3K/Akt, and MAPKs (Bloom and Jaiswal 2003; Chen et al. 2012; Weng et al. 2011). Nrf2 phosphorylation facilitates the dissociation of Nrf2 from Keap1 and Nrf2 nuclear translocation and thereby activates Nrf2-driven gene expression. It has been shown that the p38, JNK, and PI3K/Akt signaling pathways and Nrf2 are involved in quercetin-induced metallothionein expression in human hepatoma HepG2 cells (Weng et al. 2011). In addition, the ERK2/Nrf2 signaling pathway has also been shown to play a critical role in the induction of

GCLC and HO-1 gene transcription by butein and phloretin (Yang et al. 2011). In the present study, we found that chrysin phosphorylated ERK2 (Fig. 5a) and activated Nrf2 nuclear translocation (Fig. 4a), nuclear Nrf2–DNA binding activity (Fig. 4b), and ARE-driven luciferase activity (Fig. 4c). To further determine the signaling pathway and transcription factor involved in the chrysin-induced HO-1, GCLC, and GCLM expression, we used RNA interference directed against ERK2 and Nrf2. Both siNrf2 and siERK2 attenuated the chrysin-induced HO-1, GCLC, and GCLM protein expression (Figs. 4d, 5b). These results demonstrate the importance of the ERK2/Nrf2 signaling pathway in the up-regulation of HO-1, GCLC, and GCLM transcription by chrysin, apigenin, and luteolin.

Structure and function relationship studies reveal that the number and position of hydroxyl groups in the B ring is an important factor determining the potency of the inhibition by flavones of oxidation, inflammation, proliferation, and carcinogenesis and the induction of apoptosis (Chen et al. 2007; Lotito and Frei 2006; Sim et al. 2007; Ueda et al. 2004). Flavones with more hydroxyl groups have greater biological activity. For instance, the potency of the flavones in inducing tumor cell apoptosis and inhibiting proteasome activity is in the order luteolin > apigenin > chrysin (Chen et al. 2007). On the contrary, effect of the number of hydroxyl groups on the B rings of 5,7-dihydroxyflavones on regulation of CYP1 activity could not totally be explained by the difference in number of hydroxyl groups on the B ring (Kim et al. 2005). CYP1A1-mediated EROD activity was inhibited by flavones in the order luteolin > apigenin > chrysin; however, CYP1A2-dependent EROD activity was inhibited by flavones in the order chrysin > apigenin > luteolin. All of the 5,7-dihydroxyflavones showed similar inhibition of CYP1B1 activity. In the present study, chrysin and luteolin displayed greater induction of GCLC and GCLM mRNA and protein expression than did apigenin (Fig. 2a, b). Similar concentration changes in chrysin and apigenin during cell culture indicate that the differential induction of antioxidant gene expression by chrysin and apigenin is regardless of their uptake or degradation by hepatocytes (Fig. 7). The underlying mechanism for the number of hydroxyl groups on the B rings of 5,7-dihydroxyflavones in the regulation of antioxidant gene expression needs further investigation.

In conclusion, we have shown that chrysin, apigenin, and luteolin inhibit tBHP-induced oxidative stress by up-regulating HO-1, GCLC, and GCLM expression through the ERK2/Nrf2 pathway. Among the flavones studied, chrysin and luteolin exhibited greater potency in up-regulating antioxidant enzyme gene transcription than did apigenin. The antioxidant property of chrysin, apigenin, and luteolin confers them with the potential to protect against oxidative stress-mediated chronic diseases.

**Conflict of interest** The authors declare that they have no conflict of interest.

# References

Abraham NG, Kappas A (2005) Heme oxygenase and the cardiovascular-renal system. Free Radic Biol Med 39:1–25

Abraham NG, Kappas A (2008) Pharmacological and clinical aspects of heme oxygenase. Pharmacol Rev 60:79–127

Alam J, Stewart D, Touchard C, Boinapally S, Choi AM, Cook JL (1999) Nrf2, a Cap'n'Collar transcription factor, regulates induction of the heme oxygenase-1 gene. J Biol Chem 274:26071–26078

Aziz N, Munro HN (1986) Both subunits of rat liver ferritin are regulated at a translational level by iron induction. Nucleic Acids Res 14:915–927

Balla G, Jacob HS, Balla J, Rosenberg M, Nath K, Apple F, Eaton JW, Vercellotti GM (1992) Ferritin: a cytoprotective antioxidant strategem of endothelium. J Biol Chem 267:18148–18153

Biswas SK, Rahman I (2009) Environmental toxicity, redox signaling and lung inflammation: the role of glutathione. Mol Aspects Med 30:60–76

Bloom DA, Jaiswal AK (2003) Phosphorylation of Nrf2 at Ser40 by protein kinase C in response to antioxidants leads to the release of Nrf2 from INrf2, but is not required for Nrf2 stabilization/accumulation in the nucleus and transcriptional activation of antioxidant response element-mediated NAD(P)H:quinone oxidoreductase-1 gene expression. J Biol Chem 278:44675–44682

Boyle JJ, Johns M, Lo J, Chiodini A, Ambrose N, Evans PC, Mason JC, Haskard DO (2011) Heme induces heme oxygenase 1 via Nrf2: role in the homeostatic macrophage response to intraplaque hemorrhage. Arterioscler Thromb Vasc Biol 31:2685–2691

Chen D, Chen MS, Cui QC, Yang H, Dou QP (2007) Structure-proteasome-inhibitory activity relationships of dietary flavonoids in human cancer cells. Front Biosci 12:1935–1945

Chen HH, Chen YT, Huang YW, Tsai HJ, Kuo CC (2012) 4-Ketopinoresinol, a novel naturally occurring ARE activator, induces the Nrf2/HO-1 axis and protects against oxidative stress-induced cell injury via activation of PI3 K/AKT signaling. Free Radic Biol Med 52:1054–1066

Cheng WL, Lii CK, Chen HW, Lin TH, Liu KL (2004) Contribution of conjugated linoleic acid to the suppression of inflammatory responses through the regulation of the NF-kappaB pathway. J Agric Food Chem 52:71–78

Choi BM, Kim BR (2008) Upregulation of heme oxygenase-1 by brazilin via the phosphatidylinositol 3-kinase/Akt and ERK pathways and its protective effect against oxidative injury. Eur J Pharmacol 580:12–18

Clark JE, Foresti R, Green CJ, Motterlini R (2000) Dynamics of haem oxygenase-1 expression and bilirubin production in cellular protection against oxidative stress. Biochem J 348:615–619

Dinkova-Kostova AT, Talalay P (2010) NAD(P)H:quinone acceptor oxidoreductase 1 (NQO1), a multifunctional antioxidant enzyme and exceptionally versatile cytoprotector. Arch Biochem Biophys 501:116–123

Franco R, Cidlowski JA (2009) Apoptosis and glutathione: beyond an antioxidant. Cell Death Differ 16:1303–1314

Franco R, Schoneveld OJ, Pappa A, Panayiotidis MI (2007) The central role of glutathione in the pathophysiology of human diseases. Arch Physiol Biochem 113:234–258

Franklin CC, Backos DS, Mohar I, White CC, Forman HJ, Kavanagh TJ (2009) Structure, function, and post-translational regulation of the catalytic and modifier subunits of glutamate cysteine ligase. Mol Aspects Med 30:86–98

Gipp JJ, Chang C, Mulcahy RT (1992) Cloning and nucleotide sequence of a full-length cDNA for human liver gamma-glutamylcysteine synthetase. Biochem Biophys Res Commun 185:29–35

Gipp JJ, Bailey HH, Mulcahy RT (1995) Cloning and sequencing of the cDNA for the light subunit of human liver gamma-glutamylcysteine synthetase and relative mRNA levels for heavy and light subunits in human normal tissues. Biochem Biophys Res Commun 206:584–589

Ikeda H, Nishi S, Sakai M (2004) Transcription factor Nrf2/MafK regulates rat placental glutathione S-transferase gene during hepatocarcinogenesis. Biochem J 380:515–521

Itoh K, Wakabayashi N, Katoh Y, Ishii T, Igarashi K, Engel JD, Yamamoto M (1999) Keap1 represses nuclear activation of antioxidant responsive elements by Nrf2 through binding to the amino-terminal Neh2 domain. Genes Dev 13:76–86

Jansen T, Hortmann M, Oelze M, Opitz B, Steven S, Schell R, Knorr M, Karbach S, Schuhmacher S, Wenzel P, Münzel T, Daiber A (2010) Conversion of biliverdin to bilirubin by biliverdin reductase contributes to endothelial cell protection by heme oxygenase-1-evidence for direct and indirect antioxidant actions of bilirubin. J Mol Cell Cardiol 49:186–195

Kalthoff S, Ehmer U, Freiberg N, Manns MP, Strassburg CP (2010) Interaction between oxidative stress sensor Nrf2 and xenobiotic-activated aryl hydrocarbon receptor in the regulation of the human phase II detoxifying UDP-glucuronosyltransferase 1A10. J Biol Chem 285:5993–6002

Kann S, Estes C, Reichard JF, Huang MY, Sartor MA, Schwemberger S, Chen Y, Dalton TP, Shertzer HG, Xia Y, Puga A (2005) Butylhydroquinone protects cells genetically deficient in glutathione biosynthesis from arsenite-induced apoptosis without significantly changing their prooxidant status. Toxicol Sci 87:365–384

Kim HJ, Lee SB, Park SK, Kim HM, Park YI, Dong MS (2005) Effects of hydroxyl group numbers on the B-ring of 5,7-dihydroxyflavones on the differential inhibition of human CYP 1A and CYP1B1 enzymes. Arch Pharm Res 28:1114–1121

Kim YM, Pae HO, Park JE, Lee YC, Woo JM, Kim NH, Choi YK, Lee BS, Kim SR, Chung HT (2011) Heme oxygenase in the regulation of vascular biology: from molecular mechanisms to therapeutic opportunities. Antioxid Redox Signal 14:137–167

Lee HH, Park SA, Almazari I, Kim EH, Na HK, Surh YJ (2010) Piceatannol induces heme oxygenase-1 expression in human mammary epithelial cells through activation of ARE-driven Nrf2 signaling. Arch Biochem Biophys 501:142–150

Liu RM, Gao L, Choi J, Forman HJ (1998) Gamma-glutamylcysteine synthetase: mRNA stabilization and independent subunit transcription by 4-hydroxy-2-nonenal. Am J Physiol 275:L861–L869

Lopez-Lazaro M (2009) Distribution and biological activities of the flavonoid luteolin. Mini Rev Med Chem 9:31–59

Lotito SB, Frei B (2006) Dietary flavonoids attenuate tumor necrosis factor alpha-induced adhesion molecule expression in human aortic endothelial cells. Structure-function relationships and activity after first pass metabolism. J Biol Chem 281:37102–37110

Lu SC (2009) Regulation of glutathione synthesis. Mol Aspects Med 30:42–59

Moinova HR, Mulcahy RT (1998) An electrophile responsive element (EpRE) regulates beta-naphthoflavone induction of the human gamma-glutamylcysteine synthetase regulatory subunit gene. constitutive expression is mediated by an adjacent AP-1 site. J Biol Chem 273:14683–14689

Mulcahy RT, Wartman MA, Bailey HH, Gipp JJ (1997) Constitutive and beta-naphthoflavone-induced expression of the human gamma-glutamylcysteine synthetase heavy subunit gene is regulated by a distal antioxidant response element/TRE sequence. J Biol Chem 272:7445–7454

Rodella L, Lamon BD, Rezzani R, Sangras B, Goodman AI, Falck JR, Abraham NG (2006) Carbon monoxide and biliverdin prevent endothelial cell sloughing in rats with type I diabetes. Free Radic Biol Med 40:2198–2205

Rogers J, Munro H (1987) Translation of ferritin light and heavy subunit mRNAs is regulated by intracellular chelatable iron levels in rat hepatoma cells. Proc Natl Acad Sci USA 84:2277–2281

Ryter SW, Otterbein LE, Morse D, Choi AM (2002) Heme oxygenase/carbon monoxide signaling pathways: regulation and functional significance. Mol Cell Biochem 234–235:249–263

Saikawa Y, Kaneda H, Yue L, Shimura S, Toma T, Kasahara Y, Yachie A, Koizumi S (2000) Structural evidence of genomic exon-deletion mediated by Alu–Alu recombination in a human case with heme oxygenase-1 deficiency. Hum Mutat 16:178–179

Salinas M, Diaz R, Abraham NG, Ruiz de Galarreta CM, Cuadrado A (2003) Nerve growth factor protects against 6-hydroxydopamine-induced oxidative stress by increasing expression of heme oxygenase-1 in a phosphatidylinositol 3-kinase-dependent manner. J Biol Chem 278:13898–13904

Seelinger G, Merfort I, Schempp CM (2008) Anti-oxidant, anti-inflammatory and anti-allergic activities of luteolin. Planta Med 74:1667–1677

Shenvi SV, Smith EJ, Hagen TM (2009) Transcriptional regulation of rat gamma-glutamate cysteine ligase catalytic subunit gene is mediated through a distal antioxidant response element. Pharmacol Res 60:229–236

Shukla S, Gupta S (2010) Apigenin: a promising molecule for cancer prevention. Pharm Res 27:962–978

Sim GS, Lee BC, Cho HS, Lee JW, Kim JH, Lee DH, Kim JH, Pyo HB, Moon DC, Oh KW, Yun YP, Hong JT (2007) Structure activity relationship of antioxidative property of flavonoids and inhibitory effect on matrix metalloproteinase activity in UVA-irradiated human dermal fibroblast. Arch Pharm Res 30:290–298

Song IS, Tatebe S, Dai W, Kuo MT (2005) Delayed mechanism for induction of gamma-glutamylcysteine synthetase heavy subunit mRNA stability by oxidative stress involving p38 mitogen-activated protein kinase signaling. J Biol Chem 280:28230–28240

Surh YJ, Kundu JK, Na HK (2008) Nrf2 as a master redox switch in turning on the cellular signaling involved in the induction of cytoprotective genes by some chemopreventive phytochemicals. Planta Med 74:1526–1539

Terry CM, Clikeman JA, Hoidal JR, Callahan KS (1999) TNF-alpha and IL-1alpha induce heme oxygenase-1 via protein kinase C, Ca2 + , and phospholipase A2 in endothelial cells. Am J Physiol 276:H1493–H1501

Tracz MJ, Juncos JP, Grande JP, Croatt AJ, Ackerman AW, Rajagopalan G, Knutson KL, Badley AD, Griffin MD, Alam J, Nath KA (2007) Renal hemodynamic, inflammatory, and apoptotic responses to lipopolysaccharide in HO-1-/- mice. Am J Pathol 170:1820–1830

Ueda H, Yamazaki C, Yamazaki M (2004) A hydroxyl group of flavonoids affects oral anti-inflammatory activity and inhibition of systemic tumor necrosis factor-alpha production. Biosci Biotechnol Biochem 68:119–125

Weng CJ, Chen MJ, Yeh CT, Yen GC (2011) Hepatoprotection of quercetin against oxidative stress by induction of metallothionein expression through activating MAPK and PI3 K pathways and enhancing Nrf2 DNA-binding activity. N Biotechnol 28:767–777

Wu CC, Hsu MC, Hsieh CW, Lin JB, Lai PH, Wung BS (2006) Upregulation of heme oxygenase-1 by Epigallocatechin-3-gallate via the phosphatidylinositol 3-kinase/Akt and ERK pathways. Life Sci 78:2889–2897

Wung BS, Hsu MC, Wu CC, Hsieh CW (2006) Piceatannol upregulates endothelial heme oxygenase-1 expression via novel protein kinase C and tyrosine kinase pathways. Pharmacol Res 53:113–122

Xiao ZP, Peng ZY, Peng MJ, Yan WB, Ouyang YZ, Zhu HL (2011) Flavonoids health benefits and their molecular mechanism. Mini Rev Med Chem 11:169–177

Yang YM, Noh K, Han CY, Kim SG (2010) Transactivation of genes encoding for phase II enzymes and phase III transporters by phytochemical antioxidants. Molecules 15:6332–6348

Yang YC, Lii CK, Lin AH, Yeh YW, Yao HT, Li CC, Liu KL, Chen HW (2011) Induction of glutathione synthesis and heme oxygenase 1 by the flavonoids butein and phloretin is mediated

through the ERK/Nrf2 pathway and protects against oxidative stress. Free Radic Biol Med 51:2073–2081

Yao HT, Lin JH, Chiang MT, Chiang W, Luo MN, Lii CK (2011) Suppressive effect of the ethanolic extract of adlay bran on cytochrome P-450 enzymes in rat liver and lungs. J Agric Food Chem 59:4306–4314

Yet SF, Layne MD, Liu X, Chen YH, Ith B, Sibinga NE, Perrella MA (2003) Absence of heme oxygenase-1 exacerbates atherosclerotic lesion formation and vascular remodeling. FASEB J 17:1759–1761

Yu AL, Lu CY, Wang TS, Tsai CW, Liu KL, Cheng YP, Chang HC, Lii CK, Chen HW (2010) Induction of heme oxygenase 1 and inhibition of tumor necrosis factor alpha-induced intercellular adhesion molecule expression by andrographolide in EA.hy926 cells. J Agric Food Chem 58:7641–7648